



## Photocatalytic degradation of a textile dye Reactive Red 31 using phyto-synthesized titanium nanoparticles under solar irradiation

Razia Khan, M.H. Fulekar\*

*School of Environment and Sustainable Development, Central University of Gujarat, Gandhinagar, Gujarat, India, Tel. +91 8401982879; email: razia.cug@gmail.com (R. Khan), Tel. +91 9833003978; email: mhfulkar@yahoo.com (M.H. Fulekar)*

Received 5 May 2014; Accepted 25 August 2014

### ABSTRACT

In the present work, we have reported a sustainable and effective method for the degradation of a textile dye Reactive Red 31 (RR31) using synthesized titanium nanoparticles. Titanium dioxide nanoparticles were synthesized using a noxious weed, *Parthenium hysterophorus*, as reducing and capping agent for the first time. The synthesized nanoparticles were characterized and confirmed as TiO<sub>2</sub> nanoparticles by using X-ray diffraction spectroscopy, Fourier transformation infrared spectroscopy, and scanning electron microscopy analysis. A glass reactor was designed and developed for the degradation of dye under solar radiations. Photocatalytic degradation of Reactive Red 31 was carried out at different concentrations using synthesized nanoparticles. UV–vis spectroscopy, total organic carbon, and total inorganic carbon analysis were carried out for the determination of dye degradation. The results reveal that biogenic TiO<sub>2</sub> nanomaterial acts as a good photocatalyst for the degradation of textile dye Reactive Red 31.

*Keywords:* Titanium dioxide; *Parthenium hysterophorus*; XRD; Reactive Red 31; Degradation

### 1. Introduction

The release of large amounts of dyestuff containing effluents into the environment has led to serious environmental hazards. With the development of industry, a number of dyes have been extensively produced and are used in textile, printing, manufacture of paints and varnishes, manufacture of plastics, food industries, etc. [1]. Methods like chemical oxidation, ultrafiltration, adsorption, coagulation, microbial degradation, electrochemical, and photocatalytic degradation were commonly employed for the decolorization and degradation of dyes present in colored effluents. Suspended TiO<sub>2</sub> nanoparticles have been largely used

as an efficient catalyst for the decomposition of organic contaminants present in water and aqueous wastes [2].

Nanoparticles are finding wide range of applications in drug delivery, catalysis, aerospace engineering, electronics, bioremediation, biomedical sciences, gene therapy, cell targeting, and energy science. A metal oxide nanoparticle, exemplified by titanium dioxide (TiO<sub>2</sub>) is one of the most important materials for photocatalysis, cosmetics, and pharmaceuticals [3]. Higher photocatalytic efficiency of TiO<sub>2</sub> nanoparticles can be used for purification and remediation of environment and also employed for the removal of dye pollutants and biowaste organic compounds. TiO<sub>2</sub> releases free radicals such as OH, O<sub>2</sub>, HO<sub>2</sub><sup>-</sup>, and H<sub>2</sub>O<sub>2</sub> on exposure of ultraviolet irradiation [4,5]. This potent

\*Corresponding author.

oxidizing power characteristically results in degradation of organic pollutants.

The synthesis of TiO<sub>2</sub> nanoparticles has been investigated using various methods such as sol–gel, emulsion precipitation, microbial biosynthesis, and plant mediated synthesis. Preparation of nanoparticles using green technologies is advantageous over chemical agents due to their less environmental consequences. In the plant biosynthesis method, extracts from the plant may act both as reducing and capping agents in the synthesis of nanoparticles [6]. Particularly the use of latex, proteins, and phytochemicals for the synthesis of metal nanoparticles is advantageous, as it eliminates the need of cell cultures and their maintenance [7]. Recently, TiO<sub>2</sub> nanoparticles have been synthesized using natural products like *Nyctanthes arbortristis* extract, *Catharanthus roseus* leaf extract, *Eclipta prostrata* leaf extract, *Aspergillus flavus*, and *Annona squamosa* peel extract [8].

*Parthenium hysterophorus* is one of the 10 worst weeds in the world, which is a poisonous, pernicious, and aggressive weed. *Parthenium* is also known for causing toxicity and allergy in animals [9]. In this study, titanium dioxide nanoparticles are synthesized using *P. hysterophorus* leaf extract and characterized using X-ray diffraction (XRD), Fourier transformation infrared (FTIR), and scanning electron microscopy (SEM). These TiO<sub>2</sub> nanoparticles were applied for the degradation of textile dye Reactive Red 31 (RR31) in a photocatalytic reactor under solar irradiation. Analysis of degraded products was carried out using UV–vis spectrophotometry, total organic carbon (TOC), and inorganic carbon (IC).

## 2. Experiments

### 2.1. Materials

Fresh leaves of *P. hysterophorus* were collected from agricultural fields located in Gandhinagar, Gujarat, India. TiOSO<sub>4</sub> was purchased from Himedia Laboratories Pvt. Ltd, Mumbai, India. Reactive Red 31 dye was obtained from a dye manufacturing industry in Vatva G.I.D.C., Ahmedabad, Gujarat.

### 2.2. Preparation of plant extract and synthesis of nanoparticles

Aqueous extract of *P. hysterophorus* was prepared using freshly amassed leaves (20 g). Leaves were surface cleaned with running tap water, followed by washing with Milli-Q water and then boiled with 100 mL of Milli-Q water at 60°C for 5 min. This extract was filtered using Whatman No. 1 filter paper and the

filtrate so obtained was used for further experiments. For synthesis of TiO<sub>2</sub> nanoparticles, 30 mL of the aqueous extract of *P. hysterophorus* was added in 75 mL of 0.025 M TiOSO<sub>4</sub> at room temperature under stirred condition for 24 h. The TiO<sub>2</sub> nanoparticles were then purified by centrifugation. To remove sulfate ions, precipitate was washed at least three times with deionized water.

### 2.3. Characterization of nanoparticles

FTIR analysis of the dried powder of synthesized TiO<sub>2</sub> nanoparticles was carried out by Perkin–Elmer spectrum one instrumental spectrometer in attenuated total reflection mode. The sample was directly placed in the KBr crystal and the spectrum was recorded in the transmittance mode in the region of 400–4,000 cm<sup>-1</sup> at a resolution of 4 cm<sup>-1</sup>. XRD patterns of all samples were collected in the range of 10–80° (2θ) using Philips X'pert MPD instrument (CuKα radiation, λ = 1.5405 Å), operated at 40 kV and 30 mA. The morphology of the plant-synthesized TiO<sub>2</sub> nanoparticles was examined using SEM (LEO 1430 VP). Thin film of the sample was prepared on a carbon-coated copper grid by simply dropping a very small amount of the sample on the grid, and for the images it was operated at 18 kV on a 0° tilt position. Hydrodynamic size distribution of phyto-synthesized titanium dioxide nanoparticles was measured by dynamic light scattering (DLS) analysis (Zetasizer Nano ZS90, Malvern, UK).

### 2.4. Photocatalytic degradation of Reactive Red 31

Photocatalytic activity of the catalyst was evaluated by the photocatalytic degradation of Reactive Red 31 (RR31) dye (Fig. 1) in aqueous solution. Photocatalysis experiments were performed in sun light during 11:00 am to 4:00 pm on sunny days of May and June, 2013. The cylindrical reactor (Fig. 2) of 1 L capacity was made up of borosilicate glass having dimensions 150 × 75 mm (diameter × height). Photocatalytic degradation of RR 31 was carried out by taking 500 mL of 25, 50, and 75 ppm of RR31 solution in a photocatalytic reactor. A total of 0.4 g of catalyst was added per 100 mL of dye solution. Solar light was used as an energy source for catalyst excitation. The intensity of solar light was measured using Lux meter (Lutron Lx-101, Taiwan) at various time intervals of 1 h. The solution was exposed to sunlight under constant stirring. After visible light irradiation, the sample was withdrawn from the suspension at every 30 min interval during irradiation for the determination of the change in absorbance of RR31 dye.

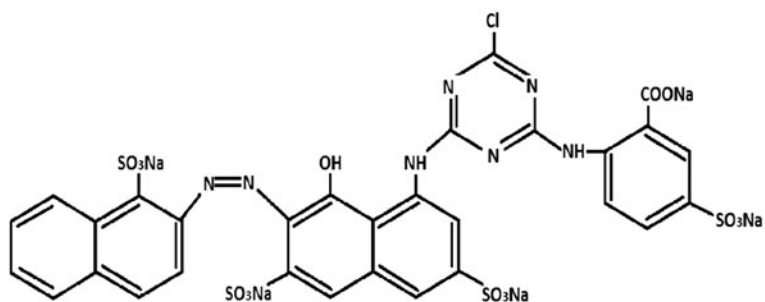


Fig. 1. Chemical structure of Reactive Red 31.

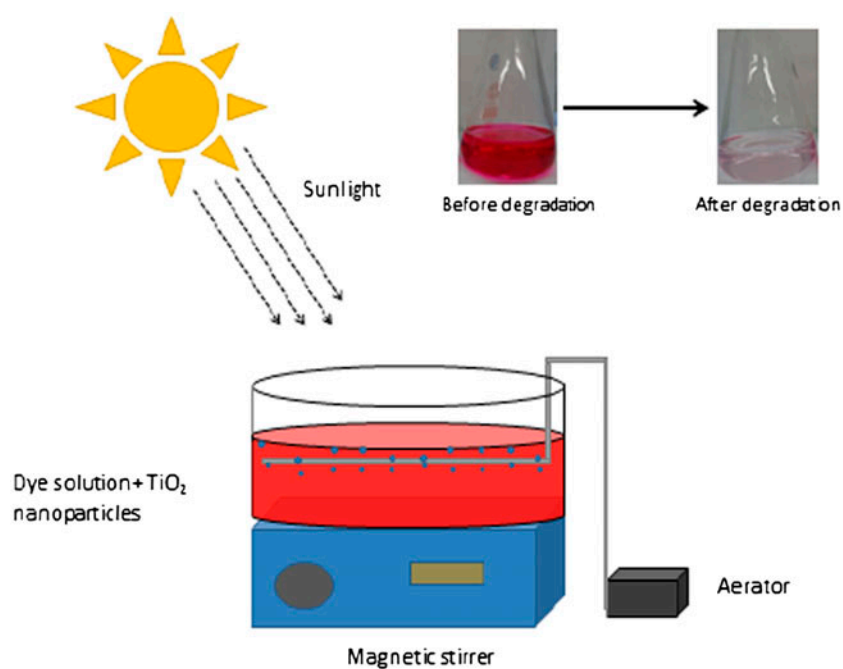


Fig. 2. Schematic diagram of photocatalytic reactor.

Decolorization efficiency of photocatalyst was determined by monitoring absorbance of RR31 at 545 nm, using UV-vis spectrophotometer (Dynamica Halo DB). Percentage of decolorization was calculated using the Eq. (1) [10];

$$\text{Decolorization (\%)} = ((AC - AT)/AC) \times 100 \quad (1)$$

where AC is the absorbance of the control and AT is the average absorbance of the test samples.

In order to evaluate the mineralization of chemical substances, TOC and IC of the samples were analyzed with a multi N/C 2000 Analytic Jena analyzer.



Fig. 3. (A) Photograph of *P. hysterophorus* leaves and (B) photograph of phyto-synthesized titanium dioxide nanoparticles.

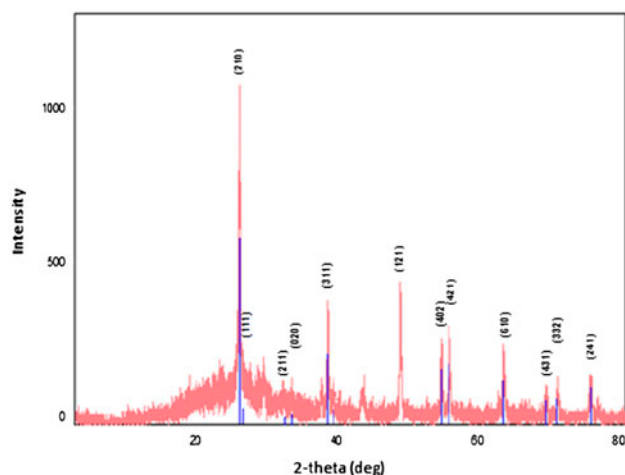


Fig. 4. XRD spectrum of *P. hysterophorus*-synthesized nanoparticles.

### 3. Results and discussion

Synthesizing  $\text{TiO}_2$  nanoparticles using an aqueous extract prepared from *P. hysterophorus* leaves (Fig. 3(A)) avoids the use of hazardous organic solvents and surfactants that are often used in chemical synthesis. Hence, in this study,  $\text{TiO}_2$  nanoparticles were synthesized by a novel, biodegradable materials, and simple green chemistry procedure using *P. hysterophorus* leaf extract. Further bio-based

fabrication is reproducible and resulting nanoparticles are hydrophilic, which enhances its applicability in bioremediation. A comparison of these results with earlier reports [11,12] indicated that enzymes/proteins, amino acids, polysaccharides, alcohols, phenols, and alkanes in *Parthenium* may be participating in the process. *P. hysterophorus* leaves contain myricyl alcohol, campesterol, stigmasterol,  $\beta$ -sitosterol, free amino acids, ursolic acid,  $2\beta$ ,  $13\alpha$ -dimethoxydihydroparthenin, salicylic acid, and protocatechuic acid [13]. Pure  $\text{TiOSO}_4$  without aqueous leaf extract of *P. hysterophorus* didn't show any color change and there was no proof for the formation of nanoparticles. After the reaction of *P. hysterophorus* extract with  $\text{TiOSO}_4$ , the color changed in to dark green (Fig. 3(B)).

The exact nature and size of the titanium nanoparticles formed were studied through XRD analysis. The XRD pattern showed the presence of broad peaks. Presence of broad peaks indicated that particles have very small crystallite sizes and are semi-crystalline in nature [14–16]. The main peak of  $\theta = 25.39^\circ$  (Fig. 4) matches the (210) crystallographic plane of brookite of  $\text{TiO}_2$  nanoparticles, indicating that nanoparticles structure dominantly correspond to brookite crystalline. There is a slight increase in the peaks which may be the result of nanoparticles synthesized by plant extract. The particles size estimation was performed by the Scherrer's equation (Eq. (2)).

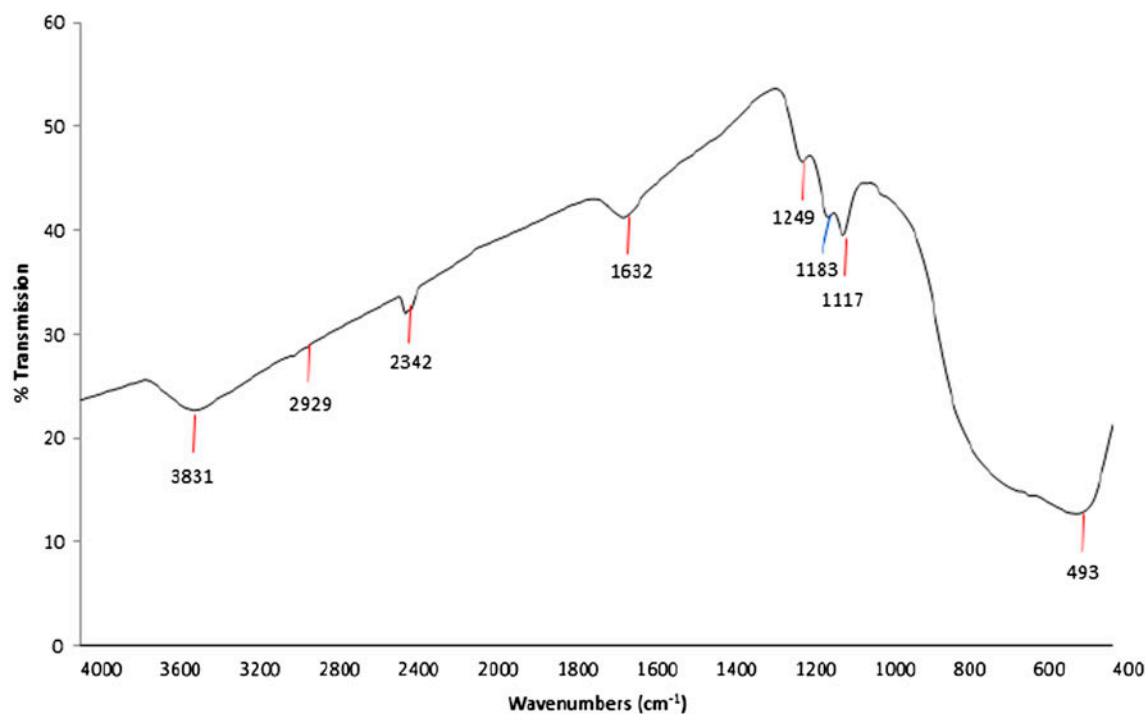


Fig. 5. FTIR spectrum of *P. hysterophorus*-synthesized nanoparticles.

$$d = 0.9\lambda/\beta\cos\theta \quad (2)$$

where  $d$  is the mean diameter of the nanoparticles,  $\lambda$  is wavelength of X-ray radiation source, and  $\beta$  is the angular FWHM of the XRD peak at the diffraction angle  $\theta$ .

The FTIR spectra of TiO<sub>2</sub> nanoparticles exhibited prominent peaks at 3,831, 2,362, 2,342, 1,632, 1,183, 1,117, 1,078, and 493 cm<sup>-1</sup> (Fig. 5). A broad peak at

3,831 cm<sup>-1</sup> shows –OH stretching vibrations. According to Hardy et al. [17] the carboxylic groups were bound to Ti–O–Ti. The band observed at 2,929 cm<sup>-1</sup> was assigned to the carboxylic groups. Peaks at 2,362 and 2,342 cm<sup>-1</sup> correspond to the band of molecular CO<sub>2</sub>. Peak at 1,632 cm<sup>-1</sup> indicates bending modes of a hydroxyl group. The band observed at 1,183 cm<sup>-1</sup> is due to bending vibration of the C–H. The peak at 1,078 is due to the Ti–O–C linkages. A broad peak 493 cm<sup>-1</sup> indicates Ti–O vibrations in the brookite

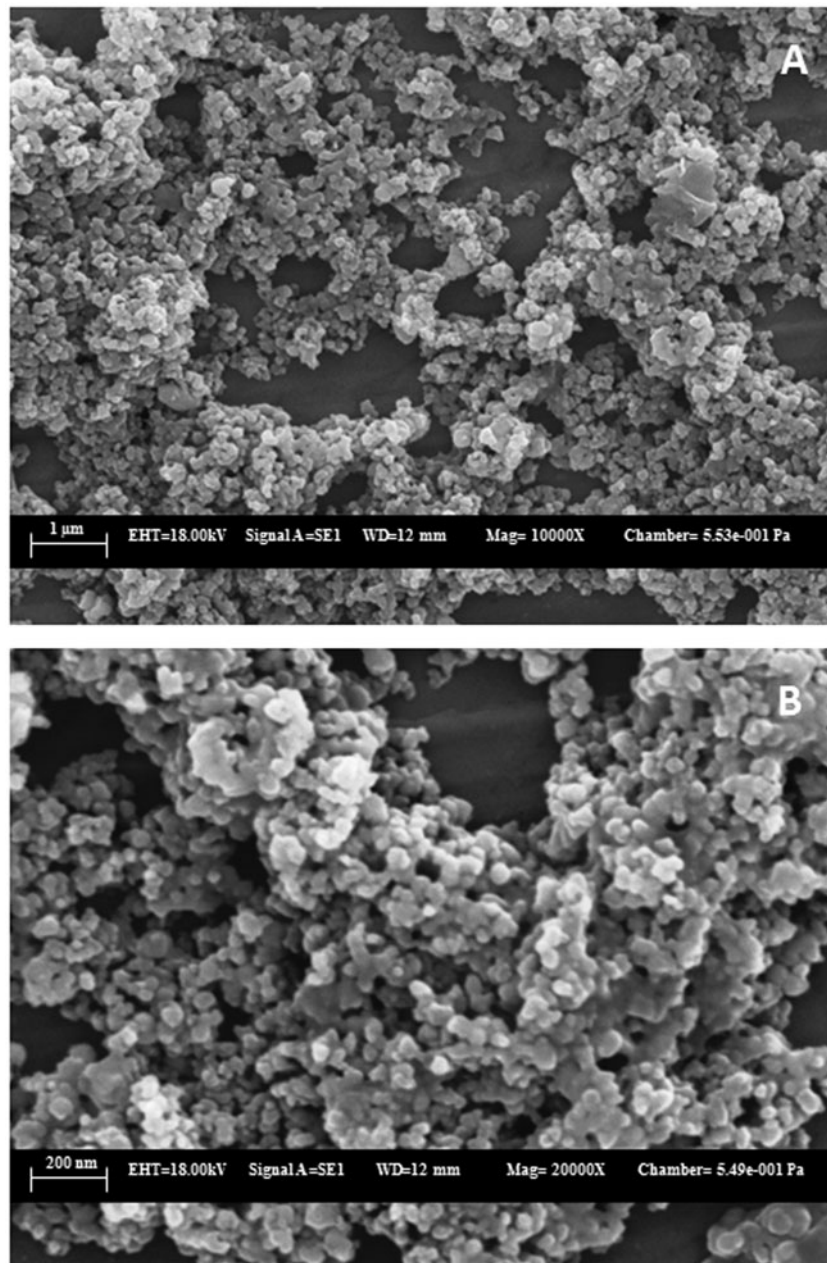


Fig. 6. SEM image of phyto-synthesized TiO<sub>2</sub> nanoparticles.

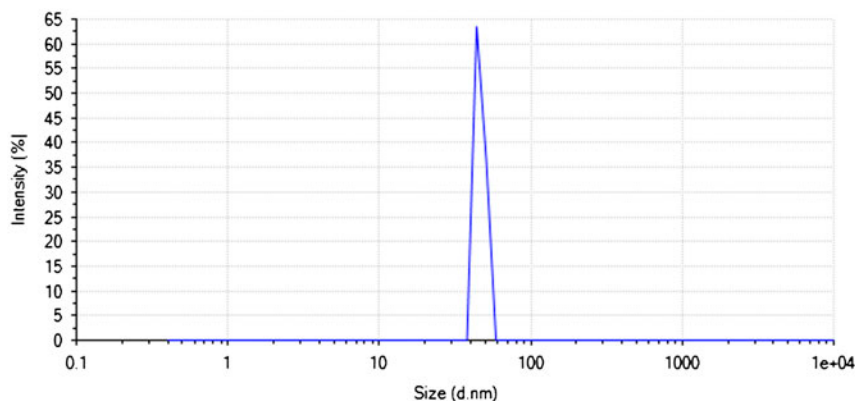


Fig. 7. DLS pattern of phyto-synthesized titanium dioxide nanoparticles.

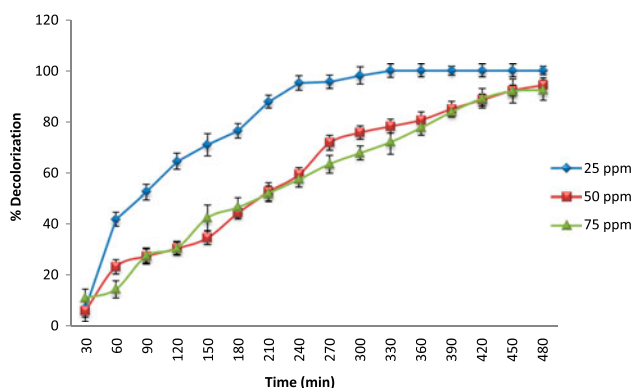


Fig. 8. Percentage decolorization of RR31 dye at different dye concentrations.

phase of  $\text{TiO}_2$ . Mandal et al. [18] proposed that the proteins could bind with nanoparticles either through free amine groups or crystalline residues in the proteins. The carboxylic groups are known to coordinate with metal ions, which may act as a nucleation site for nanoparticle formation [19–21].

The surface morphology of synthesized nanoparticles was investigated using SEM. The SEM images of the *P. hysterophorus*-synthesized  $\text{TiO}_2$  nanoparticles have shown spherical clusters of the nanoparticles (Fig. 6). Phyto-synthesized  $\text{TiO}_2$  nanoparticles were spherical, oval in shape, agglomerated, as well as quite polydisperse, and ranges in size from 13 to 56 nm. The observed DLS Z-average diameter was 54.86 dnm (Fig. 7) which was similar to the results of SEM and XRD analysis.

The photocatalytic activity of bio-synthesized  $\text{TiO}_2$  nanoparticles was tested for the degradation of Reactive Red 31 in sunlight. Intensity of solar radiations was found to be between 780,000 and 958,000 lux. Results of RR31 degradation by using synthesized

$\text{TiO}_2$  as catalyst prepared by green method was presented in Figs. 8–10. From the results of our study, it was found that the catalyst shows least efficiency towards photocatalytic degradation of RR31 at 75 ppm (92.34%), as compared to 25 (100%) and 50 ppm (94.25%) of the dye (Fig. 8) after 8 h. It was also observed that catalytic activity gradually decreased by increasing dye concentration. Decrease in catalytic activity of  $\text{TiO}_2$  at higher dye concentration as compared to lower concentrations is due to the higher availability of dye molecules for degradation in the presence of constant catalyst concentration.

The UV–vis scan of the control (25, 50, and 75 ppm dye) and decolorized solution was performed. UV–vis analysis of control containing RR31 dye showed gradual reduction and final disappearance of peaks at 287 and 545, when treated using titanium nanoparticles under solar radiation. The disappearance of the peaks at 287 and 545 nm after 8 h implies that the synthetic dye has been degraded at various dye concentrations (Fig. 9). The decolorized sample showed disappearance of the peaks in both UV and visible regions. To support this data, TOC and IC content of control (25, 50, and 75 ppm dye) and decolorized solution was also performed. With the decrease in TOC content, an increase in IC content was observed (Fig. 10). This was observed may be due to mineralization of dye present in the solution due to the photocatalytic activity of  $\text{TiO}_2$  under solar radiations. Also, with the increase in dye concentration, decrease in % reduction of TOC was observed. Similar results were reported by Patel et al. [22].

During the photocatalytic process, absorption of photons by the photocatalyst leads to excitations of electrons from the valance band to the conduction band, generating electrons/hole pairs. Electrons in the conduction band were probably captured by  $\text{O}_2$

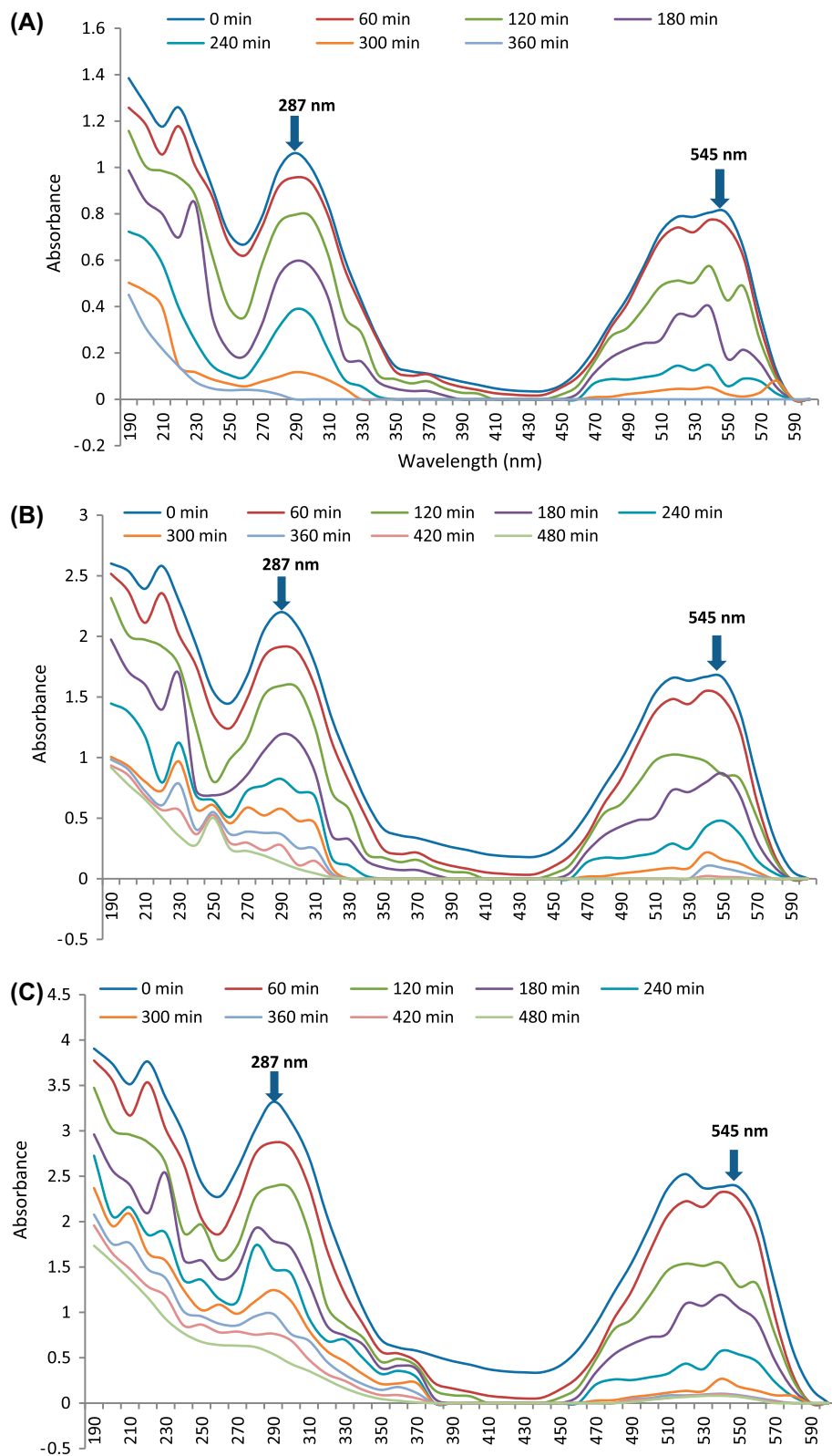


Fig. 9. UV-vis scanning of degraded dye product at 25 ppm (A), 50 ppm (B), and 75 ppm (C) for different time intervals.

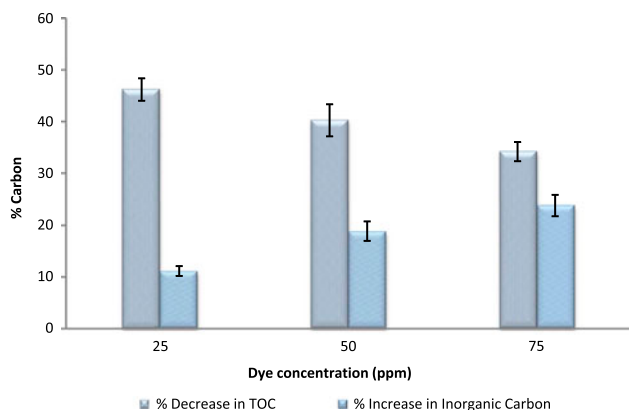


Fig. 10. Percent increase or decrease in organic and IC of degraded dye compound at various concentrations.

molecules dissolved in the suspension and in the valance band captured by  $\text{OH}^-$  or  $\text{H}_2\text{O}$  species absorbed on the surface of the catalyst to produce hydroxyl radicals. Those hydroxyl radicals then oxidize the dye. Thus, recombination of photogenerated electrons and holes is one of the most significant factors that determines the photocatalytic activity of phyto-synthesized  $\text{TiO}_2$  nanoparticles [23].

#### 4. Conclusions

There is a critical need for the development of reliable, sustainable, and effective approach for the treatment of dyestuff-containing effluents. Here, we have reported a simple, ecofriendly, and low-cost approach for the degradation of Reactive Red 31 using  $\text{TiO}_2$  nanoparticles under solar irradiation. Titanium nanoparticles were synthesized by a green synthesis method using an aqueous extract of *P. hysterophorus* leaves as a reducing and capping agent. Titanium nanoparticles prepared by this green method exhibited higher visible light activities at lower dye concentrations as compared to higher dye concentrations. This nanotechnological approach is a rapid and better alternative for the remediation of dyestuff containing effluents.

#### References

[1] R. Khan, Z. Khan, B. Nikhil, D. Jyoti, M. Datta, Azo dye decolorization under microaerophilic conditions by a bacterial mixture isolated from anthropogenic dye-contaminated soil, *Biorem. J.* 18 (2014) 147–157.  
 [2] K. Pirkanniemi, M. Sillanpää, Heterogeneous water phase catalysis as an environmental application: A review, *Chemosphere* 48 (2002) 1047–1060.  
 [3] A.V. Kirthi, A.A. Rahuman, G. Rajakumar, S. Marimuthu, T. Santhoshkumar, C. Jayaseelan,

G. Elango, A.A. Zahir, C. Kamaraj, A. Bagavan, Biosynthesis of titanium dioxide nanoparticles using bacterium *Bacillus subtilis*, *Mater. Lett.* 65 (2011) 2745–2747.  
 [4] C. Jayaseelan, A.A. Rahuman, S.M. Roopan, A.V. Kirthi, J. Venkatesan, S.K. Kim, M. Iyappan, C. Siva, Biological approach to synthesize  $\text{TiO}_2$  nanoparticles using *Aeromonas hydrophila* and its antibacterial activity, *Spectrochim. Acta, Part A* 107 (2013) 82–89.  
 [5] A.S. Roy, A. Parveen, A.R. Koppalkar, M.V.N.A. Prasad, Effect of nano-titanium dioxide with different antibiotics against methicillin-resistant *Staphylococcus aureus*, *J. Biomater. Nanobiotechnol.* 1 (2010) 37–41.  
 [6] G. Rajakumar, A.A. Rahuman, S.M. Roopan, V.G. Khanna, G. Elango, C. Kamaraj, A.A. Zahir, K. Velayutham, Fungus-mediated biosynthesis and characterization of  $\text{TiO}_2$  nanoparticles and their activity against pathogenic bacteria, *Spectrochim. Acta, Part A* 91 (2012) 23–29.  
 [7] M. Hudlikar, S. Joglekar, M. Dhaygude, K. Kodam, Green synthesis of  $\text{TiO}_2$  nanoparticles by using aqueous extract of *Jatropha curcas* L. latex, *Mater. Lett.* 75 (2012) 196–199.  
 [8] S.M. Roopan, A. Bharathi, A. Prabhakarn, A.A. Rahuman, K. Velayutham, G. Rajakumar, R.D. Padmaja, M. Lekshmi, G. Madhumitha, Efficient phyto-synthesis and structural characterization of rutile  $\text{TiO}_2$  nanoparticles using *Annona squamosa* peel extract, *Spectrochim. Acta, Part A* 98 (2012) 86–90.  
 [9] P. Rajiv, S. Rajeshwari, R. Venckatesh, Bio-fabrication of zinc oxide nanoparticles using leaf extract of *Parthenium hysterophorus* L. and its size-dependent antifungal activity against plant fungal pathogens, *Spectrochim. Acta, Part A* 112 (2013) 384–387.  
 [10] R.G. Saratale, G.D. Saratale, D.C. Kalyani, J.S. Chang, S.P. Govindwar, Enhanced decolorization and biodegradation of textile azo dye Scarlet R by using developed microbial consortium-GR, *Bioresour. Technol.* 100 (2009) 2493–2500.  
 [11] D. Inbakandan, R. Venkatesan, S. Ajmal Khan, Biosynthesis of gold nanoparticles utilizing marine sponge *Acanthella elongata* (Dendy, 1905), *Colloids Surf., B* 81 (2010) 634–639.  
 [12] G. Rajakumar, A. Abdul Rahuman, B. Priyamvada, V. Gopiesh Khanna, D. Kishore Kumar, P.J. Sujin, *Eclipta prostrata* leaf aqueous extract mediated synthesis of titanium dioxide nanoparticles, *Mater. Lett.* 68 (2012) 115–117.  
 [13] M. Khan, S. Ahmad, Pharmacognostical, phytochemical, biological and tissue culture studies on *Parthenium hysterophorus* Linn.: A review, *Int. J. Altern. Med.* 6(2) (2008) 5–9.  
 [14] M. Moroni, D. Borrini, L. Calamai, L. Dei, Ceramic nanomaterials from aqueous and 1, 2-ethanediol supersaturated solutions at high temperature, *J. Colloid Interface Sci.* 286 (2005) 543–550.  
 [15] Y. Wang, A. Zhou, Z. Yang, Preparation of hollow  $\text{TiO}_2$  microspheres by the reverse microemulsions, *Mater. Lett.* 62 (2008) 1930–1932.  
 [16] C. Jayaseelan, A.A. Rahuman, S.M. Roopan, A.V. Kirthi, J. Venkatesan, S.K. Kim, M. Iyappan, C. Siva, Biological approach to synthesize  $\text{TiO}_2$  nanoparticles using *Aeromonas hydrophila* and its antibacterial activity, *Spectrochim. Acta, Part A* 107 (2013) 82–89.

- [17] A. Hardy, J.D. Haen, M.K.V. Bael, J. Mullens, An aqueous solution–gel citratoperoxo–Ti(IV) precursor: Synthesis, gelation, thermo-oxidative decomposition and oxide crystallization, *J. Sol-Gel Sci. Technol.* 44 (2007) 65–74.
- [18] D. Mandal, M.E. Bolander, D. Mukhopadhyay, G. Sarkar, P. Mukherjee, The use of microorganisms for the formation of metal nanoparticles and their application, *Appl. Microbiol. Biotechnol.* 69 (2006) 485–492.
- [19] R.T. Clay, R.E. Cohen, Synthesis of metal nanoclusters within microphase separated diblock copolymers: Sodium carboxylate vs carboxylic acid functionalization, *Supramol. Sci.* 5 (1998) 41–48.
- [20] S. Joly, R. Kane, L. Radzilowski, T. Wang, A. Wu, R.E. Cohen, E.L. Thomas, M.F. Rubner, Multilayer nanoreactors for metallic and semiconducting particles, *Langmuir* 16 (2000) 1354–1359.
- [21] P. Dhandapani, S. Maruthamuthu, G. Rajagopal, Bio-mediated synthesis of TiO<sub>2</sub> nanoparticles and its photocatalytic effect on aquatic biofilm, *J. Photochem. Photobiol., B* 110 (2012) 43–49.
- [22] V.R. Patel, N.S. Bhatt, H.B. Bhatt, Involvement of ligninolytic enzymes of *Myceliophthora vellerea* HQ871747 in decolorization and complete mineralization of Reactive Blue 220, *Chem. Eng. J.* 233 (2013) 98–108.
- [23] G.K. Naik, P.M. Mishra, K. Parida, Green synthesis of Au/TiO<sub>2</sub> for effective dye degradation in aqueous system, *Chem. Eng. J.* 229 (2013) 492–497.